This article was downloaded by: [National Science Library]
On: 04 August 2015, At: 18:15
Publisher: Taylor & Francis
Informa Ltd Registered in England and Wales Registered Number: 1072954 Registered office: 5 Howick Place, London, SW1P 1WG

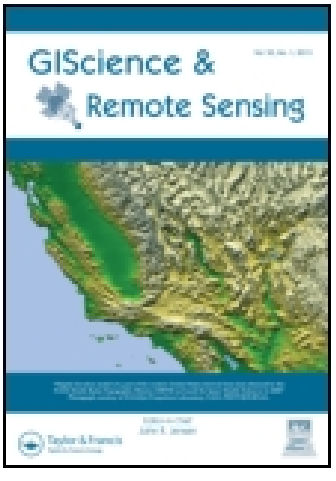


CrossMark
Click for updates

GIScience & Remote Sensing
Publication details, including instructions for authors and subscription information:
http://www.tandfonline.com/loi/tgrs20

# The responses of vegetation water content (EWT) and assessment of drought monitoring along a coastal region using remote sensing

Zhiqiang Gao[a], Qiuxian Wang[a], Xiaoming Cao[b] & Wei Gao[c]

[a] Yantai Institute of Coastal Zone Research, Chinese Academy of Science, Yantai, 264003, China

[b] Institute of Desertification Studies, Chinese Academy of Forestry, Beijing, 100101, China

[c] USDA UVB Monitoring and Research Program, Natural Resource Ecology Laboratory, Colorado State University, Fort Collins, CO, 80525, USA

Published online: 17 Feb 2014.

To cite this article: Zhiqiang Gao, Qiuxian Wang, Xiaoming Cao & Wei Gao (2014) The responses of vegetation water content (EWT) and assessment of drought monitoring along a coastal region using remote sensing, GIScience & Remote Sensing, 51:1, 1-16, DOI: 10.1080/15481603.2014.882564

To link to this article: http://dx.doi.org/10.1080/15481603.2014.882564

PLEASE SCROLL DOWN FOR ARTICLE

Taylor & Francis makes every effort to ensure the accuracy of all the information (the "Content") contained in the publications on our platform. However, Taylor & Francis, our agents, and our licensors make no representations or warranties whatsoever as to the accuracy, completeness, or suitability for any purpose of the Content. Any opinions and views expressed in this publication are the opinions and views of the authors, and are not the views of or endorsed by Taylor & Francis. The accuracy of the Content should not be relied upon and should be independently verified with primary sources of information. Taylor and Francis shall not be liable for any losses, actions, claims, proceedings, demands, costs, expenses, damages, and other liabilities whatsoever or howsoever caused arising directly or indirectly in connection with, in relation to or arising out of the use of the Content.

This article may be used for research, teaching, and private study purposes. Any substantial or systematic reproduction, redistribution, reselling, loan, sub-licensing, systematic supply, or distribution in any form to anyone is expressly forbidden. Terms &

Conditions of access and use can be found at http://www.tandfonline.com/page/terms-and-conditions

Downloaded by [National Science Library] at 18:15 04 August 2015

*GIScience & Remote Sensing*, 2014
Vol. 51, No. 1, 1–16, http://dx.doi.org/10.1080/15481603.2014.882564

Taylor & Francis
Taylor & Francis Group

# The responses of vegetation water content (EWT) and assessment of drought monitoring along a coastal region using remote sensing

Zhiqiang Gao[a], Qiuxian Wang[a], Xiaoming Cao[b]* and Wei Gao[c]

[a]*Yantai Institute of Coastal Zone Research, Chinese Academy of Science, Yantai, 264003, China;* [b]*Institute of Desertification Studies, Chinese Academy of Forestry, Beijing, 100101, China;* [c]*USDA UVB Monitoring and Research Program, Natural Resource Ecology Laboratory, Colorado State University, Fort Collins, CO, 80525, USA*

(*Received 18 June 2013; accepted 19 November 2013*)

This article retrieved the vegetation water content equivalent water thickness (EWT) information and the relevant parameters for the land surface from full-band TM remote sensing data. The effects of surface water heat flux and surface covering on the EWT were analyzed via studies of the regional land cover status and the combined EWT with land surface parameters. This article also analyzed the roles and limitations of EWT in drought monitoring combined with classification of the regional drought and regional water stress index (RWSI). From the results, the following conclusions were reported. (1) The spatial distribution of the EWT is closely related to the vegetation, and the EWT is able to monitor the regional water conditions to a certain extent. (2) The distribution of the EWT is affected significantly by the density of vegetation cover, land surface temperature and evapo-transpiration. (3) The correlation between the NDVI (or fractional vegetation cover) and the EWT differs under different vegetation coverage conditions. (4) The evapo-transpiration of the ecological environment is closely tied to the EWT such that the changes in evapo-transpiration affect the EWT significantly. (5) The ability of the EWT to monitor regional drought is conditional, and therefore no significant indication exists that can be used to monitor moderate to severe drought conditions.

**Keywords:** equivalent water thickness (EWT); land surface parameters; remote sensing; responses

Downloaded by [National Science Library] at 18:15 04 August 2015

## 1. Introduction

Monitoring of vegetation water not only aids in understanding the conditions for plant growth but also plays an indispensable role in assessing the risk of forest fire, monitoring of drought conditions and ecological security and evaluating regional water resources. Many specialists have studied the definition of vegetation water content in detail and have suggested several indices for vegetation water content, such as the relative water content (RWC), relative drought index (RDI), fuel moisture content (FMC) and equivalent water thickness (EWT). Among these indices, the EWT is defined as the ratio of the vegetation water content and its total leaf area (Dawson, Curran, and Plummer 1998), and the EWT can be revised using the leaf area index (Ceccato et al. 2001) to describe the vegetation water content more accurately. The FMC is affected by the dry matter in the leaves (Ceccato, Flasse, and Gregoire 2002; Ceccato et al. 2002). Therefore, this article adopts the coupling of the EWT and the FMC for further study of the vegetation water content.

*Corresponding author. Email: caoxm1027@gmail.com

© 2014 Taylor & Francis

With its advantages, remote sensing technology has become an important means for monitoring the vegetation water content over the long term and large scale. Early in the 1970s, many scientists across the world began to focus on monitoring of vegetation water content using remote sensing. Tucker (1977) first proposed a method for retrieving the vegetation water content using the reflectance of the near-infrared band after studying the foliar spectral reflection characteristics. Currently, researchers at home and abroad have put forth many methods for retrieving the vegetation water content by means of remote sensing. In summary, the main approaches include the dielectric constant based on radar data; the vegetation index based on multispectral data, chlorophyll and vegetation status; statistical analysis and the radiative transfer model.

Using airborne synthetic aperture radar (AIRSAR) data, Moghaddam and Saatchi (1999) accessed the dielectric constant information from canopy vegetation on the surface of a boreal forest area and the vegetation water content was subsequently retrieved based on the empirical relationship between the permittivity and vegetation water. The long-band microwave radiation is able to penetrate not only the clouds but also the vegetation and even the soil to a certain extent, but this empirical method may result in errors in retrieving the vegetation water content.

The vegetation index method based on the chlorophyll content assumes that the chlorophyll content of vegetation is proportional to the vegetation water content. Thus, the vegetation water content may be retrieved using the indirect relationship with the vegetation indices. Currently, there are also certain indices available for retrieving the vegetation water content, such as the RGI (relative greenness index) and GEMI (global environment monitoring index), which assess the risk of forest and grassland fires. In later studies, however, researchers realized that this view was unilateral. The chlorophyll content of certain species is influenced not only by the vegetation water but also by factors of phenology status, atmospheric pollution, nutrient supply, toxic elements, vegetation pests, diseases and radiation stress, among others. Therefore, it is not sufficiently accurate to use the chlorophyll content to retrieve the vegetation water information for these species (Tucker 1977). Moreover, the chlorophyll content of certain species in nature is independent of vegetation water. For example, Gobron et al. (1999) discovered five plants in which the chlorophyll content had no relationship with its vegetation water in a temperate humid forest.

The vegetation status is an indicator that reflects the vegetation as influenced by the environment. Chuvieco et al. (2001) stated that the vegetation water content could drive the difference in temperature between the air and the leaf surface, which may aid in calculation of the vegetation water content for the study of the dynamic changes in vegetation heat. Based on this theory, certain indices for measuring evapo-transpiration were proposed, such as the crop–water stress index (CWSI), water deficit index (WDI), the stress index (SI), etc., and these indices can be used to assess the vegetation state (Peng, Chen, and Li 2007).

Dr. Dawson thought that the water index (WI) proposed by Penuelas et al. and the normalized difference water index (NDWI) proposed by Gao (1996) showed a good direct correlation with the EWT. Additionally, the physical or semi-empirical method coupled with the radiative transfer model can simulate the effect of vegetation water on the reflectivity. Currently, the main physical models used to retrieve the vegetation water content are the leaf optical model based on the radiative transfer equation known as PROSPECT, the canopy model referred to as SAIL and their various coupling models (Wang, Xu, and Ma 2008; Pietro Ceccato et al. 2001; Brown et al. 2008; Finn et al. 2013).

Downloaded by [National Science Library] at 18:15 04 August 2015

Therefore, this article retrieved the EWT over different ecosystems using TM remote sensing data. Using studies on the regional land-cover status, the effects of surface water/heat flux and land-cover on the EWT were analyzed by combining the EWT with other land surface parameters (such as the fractional vegetation cover (FVC), NDVI, land surface temperature (LST), ET, etc.). The roles and limitations of the EWT in drought monitoring were studied by combining the classifications of the regional drought status and the regional water stress index (RWSI).

## 2. Materials and methods

### 2.1. The study area

The study area is located at Laizhou Bay in Shandong Province, China (Figure 1) within the latitude of 36° 48′ 43″–37° 32′ 49″ and longitude 118° 37′ 37″–119° 44′ 31″. The length along the east–west and of north–south directions is approximately 97 and 79 km, respectively. The total study area is 486,245 ha. Land elevation drops mildly from 30 to 2 m above the sea level. Yet the length of the meandering coastal line within the study area is about 400 km. Such coastal region is an active floodplain that was formed by sediment laden water being released from the neighboring river channel through the regional morphological and sedimentary dynamics. Three cities, including the Shouguang City, part of the Weifang City (i.e. the Hangting area) and most of the Changyi City, are situated along this coastal line. The sediment distribution in the alluvial plain ranges from fine sand (close to the low water line) to the typical mud carried by flood currents. Close to the open ocean, the climate system in this area is a moist, warm, temperate continental monsoon climate (Cao 2002; Wang, Ren, and Sun 2002).

### 2.2. The satellite image processing

First of all, Landsat TM images, digital elevation model (DEM) data and climate data were collected. All datasets were vectorized and interpolated as grid datasets with UTM projection in advance to ease the application in geographical information systems (GIS).

In this study, the raw images were geo-referenced to a common UTM coordinate system, and we then re-sampled all of the images to unify relative resolution in images of

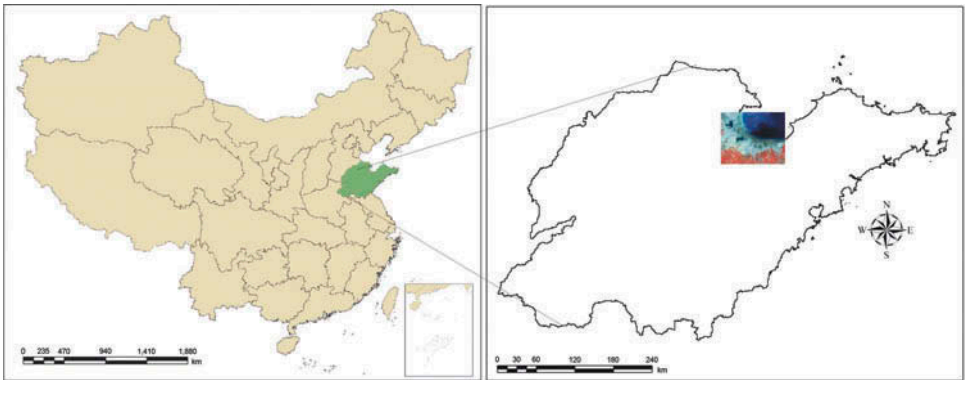

Figure 1. The location of the study area in Shandong Province, China.

Downloaded by [National Science Library] at 18:15 04 August 2015

different sizes using the nearest neighbor algorithm with a pixel size of 30 m by 30 m for all bands, including the thermal band.

Landsat TM/ETM+ images were processed for the mapping of land use/land cover change (LUCC), VIs, LST and heat fluxes. LUCC associated with 7 May 1987 in the study area was analyzed with respect to the proper interpretation of Landsat TM image and was validated with ground truth data. Regional scale ET and heat fluxes were estimated with the aid of remote sensing images and the surface energy balance algorithm (e.g. SEBAL model) (Bastiaanssen, Menenti, and Feddes 1998; Bastiaanssen, Pelgrum, and Wang 1998). LST retrieval was carried out using the thermal bands of TM/ETM+ data to ease the application of the Radiance Transfer Equation (Qin, Karnieli, and Berliner 2001). The equations for normalized difference vegetation index (NDVI) (Rouse et al. 1973; Tucker 1979), FVC (Gutman and Ignatov 1998) were collectively employed to produce a suite of VIs in support of vegetation water impact assessment. All of the preparatory efforts led to develop the integrated TVDI and RWSI for final analysis in the context of vegetation water. The following subsections will introduce these algorithms/equations in a greater detail.

### 2.3. The retrieval of vegetation water content information (GVMI and EWT)

Because both the near-infrared and the short-wave infrared bands are more sensitive to changes in the vegetation water content, the Global Vegetation Moisture Index (GVMI) is chosen to retrieve the vegetation water content and the formula is expressed as follows (1):

$$\mathrm{GVMI} = \frac{(\mathrm{NIR} + 0.1) - (\mathrm{SWIR} + 0.02)}{(\mathrm{NIR} + 0.1) + (\mathrm{SWIR} + 0.02)} \tag{1}$$

where NIR is the near-infrared reflectance (band range: 0.79–0.89 μm) and the SWIR is the shortwave infrared reflectance (band range: 0.58–1.75 μm).

The quantitative relationship between the GVMI and EWT is established according to Ceccato, Flasse, and Gregoire (2002) and Ceccato et al. (2002) via a fitting method and field measurement data formula is expressed as follows:

$$\mathrm{GVMI} = a + \frac{b}{1 + d\left(\mathrm{EWT}_{\mathrm{canopy}}\right)} + c\left(\mathrm{EWT}_{\mathrm{canopy}}\right) \tag{2}$$

where $a = 1.53$, $b = -1.40$, $c = -0.000099$ and $\mathrm{EWT}_{\mathrm{canopy}}$ is vegetation water content. Later, to test on the actual application effect of the formula, Ceccato, Flasse, and Gregoire (2002) and Ceccato et al. (2002) found that significant differences exist between the formula calculation results and the field measurement data, but their regression lines were parallel. Ceccato thought that systematic errors in the sensor and measurement tools led to the generation of this error, and thus they introduced a constant into the formula to reduce the error. The revised formula (2) is expressed as

$$\mathrm{GVMI} = a + \frac{b}{1 + d\left(\mathrm{EWT}_{\mathrm{canopy}}\right)} + c\left(\mathrm{EWT}_{\mathrm{canopy}}\right) - 0.13 \tag{3}$$

Downloaded by [National Science Library] at 18:15 04 August 2015

and the formula of the $EWT_{canopy}$ can be derived from Equation (3), as shown in Equation (4).

$$EWT_{canopy} = -\frac{ad + c - d(GVMI + 0.13)}{2cd} + \frac{\sqrt{(ad + c - d(GVMI + 0.13))^2 - 4cd(a + b - GVMI - 0.13)}}{2cd} \quad (4)$$

where $a$ = 1.53, $b$ = –1.40, $c$ = –0.000099, $d$ = 0 .000517 and $r^2$ is the judgment coefficient or $r^2 = 0.87$, $p < 0.001$. Because the base of the extracting square root should be greater than 0, we calculated the GVMI in the range [0, 0.556], and the corresponding $EWT_{canopy}$ range is [0, 3295.76].

### 2.4. The retrieval of other related parameters

#### 2.4.1. Retrieval of the land surface heat fluxes, ET and LST

The heat fluxes in this study were estimated from the Landsat satellite images using the SEBAL model and were calculated using Arc/Info 9.0 Macro Language (AML) and Compaq Visual FORTRAN 6.5 mixed-language programming (Bastiaanssen, Menenti, and Feddes 1998; Bastiaanssen, Pelgrum, and Wang 1998; Gao et al. 2010). Our SEBAL-based computer package operated in a Microsoft Windows system using the ESRI GRID module as the major data format. To ease application of the radiance transfer equation, Qin, Karnieli, and Berliner (2001) derived an approximate expression for LST retrieval that is suitable for the thermal bands of the TM/ETM+ data. Our LST maps were also derived based on the same algorithm developed by Qin, Karnieli, and Berliner (2001).

#### 2.4.2. Calculations for the NDVI and FVC

The equation for the NDVI (Rouse et al. 1973; Tucker 1979) is summarized as follows:

$$NDVI = \frac{\rho_{nir} - \rho_{red}}{\rho_{nir} + \rho_{red}} \quad (5)$$

where $\rho_{red}$ is the red band (0.63–0.69 μm) reflectance, and $\rho_{nir}$ is the near red band (0.76–0.90 μm) reflectance.

The calculation of the FVC is based on the NDVI values, which may be calculated using the spectral reflectance data. The atmospheric correction of the Landsat TM/ETM data was conducted with a combination of the look up table (LUT) and dark-object method (DOM) (Kaufman and Sendra 1988, Kaufman et al. 1997; Kaufman, Karnieli, and Tanre 2000; Liang et al. 1997, 2002; Liang, Fang, and Chen 2001). The algorithm developed by Gutman and Ignatov (1998) was applied to compute the FVC as expressed below:

$$FVC = \frac{I_{NDVI} - I_{NDVI,s}}{I_{NDVI,v} - I_{NDVI,s}} \quad (6)$$

Downloaded by [National Science Library] at 18:15 04 August 2015

where FVC is the fractional vegetation cover (%), $I_{NDVI}$ is the NDVI value at each pixel (dimensionless), $I_{NDVI,v}$ is the NDVI value that corresponds to 100% vegetation cover (dimensionless) and $I_{NDVI,s}$ is the NDVI of bare soil (dimensionless).

#### 2.4.3. Calculations of the regional water stress index (RWSI) and temperature vegetation dryness index (TVDI)

According to the CWSI mechanism (Jackson and Idso 1981), this study defines the RWSI as follows:

$$\mathrm{RWSI} = 1 - \frac{\lambda ET}{\lambda ET_{\mathrm{wet}}} = \frac{H}{R_n - G} \tag{7}$$

where ET is the regional actual ET ($m^2\ ha^{-1}\ day^{-1}$) and $ET_{wet}$ is the regional potential ET ($m^2\ ha^{-1}\ day^{-1}$). The SEBAL model can be used to generate the relevant heat fluxes ($H$, $R_n$ and $G$), $H$ is the sensible heat flux ($W/m^2$), $R_n$ is the net radiation flux ($W/m^2$) and $G$ is the soil heat flux ($W/m^2$) (Bastiaanssen, Menenti, and Feddes 1998; Bastiaanssen, Pelgrum, and Wang 1998; Gao et al. 2010). Therefore, the regional water deficit can be monitored on a near real-time basis with the aid of remote sensing technologies.

Sandholt, Rasmussen, and Andersen (2002) noted that the simplified triangle space of the LST–NDVI may exhibit soil moisture contours reflecting the spatial patterns of the vegetation index/temperature trapezoid eigenspace (VITT) (see Figure 2), which led to the definition of the TVDI as expressed below:

$$\mathrm{TVDI} = \frac{Ts - Ts_{\min}}{Ts_{\max} - Ts_{\min}} \tag{8}$$

where $Ts_{min}$ is the minimum LST given the NDVI along the wet edge (K) (see Figure 2), $Ts_{max}$ is the maximum LST given the NDVI along the dry edge (K) (see Figure 2) and $Ts$is the LST in any given pixel (K) (see Figure 2).

## 3. Results and discussion

We selected the remote sensing TM images of seven bands in the study area on 7 May 1987 and retrieved the EWT as case study. Next, using the false color images generated from the fourth, third and second bands, we extracted the land cover information of the study area by artificial visual interpretation and retrieved the FVC, NDVI, LST, RWSI, ET, TVDI, and EWT and related land surface information with the infrared, near-infrared and shortwave infrared bands. The information presented in the results and discussion was analyzed using the above indices.

### 3.1. Spatial distribution analysis of EWT and other surface parameters

The Landsat TM data were used for analysis of the LULC. With the aid of actual ground data throughout the calibration and validation stages, the findings clearly indicate that the LULC can be classified into seven categories: farmland, grassland, woodland, water bodies, beach land, built-up land and saline-alkali land. As shown in Figure 3, farmland accounted for 44.9% of the total area, followed by water bodies and saline-alkali land, which accounted for 20.4% and 17.1% of the total area, respectively. Built-up land (cities,

Downloaded by [National Science Library] at 18:15 04 August 2015

Downloaded by [National Science Library] at 18:15 04 August 2015

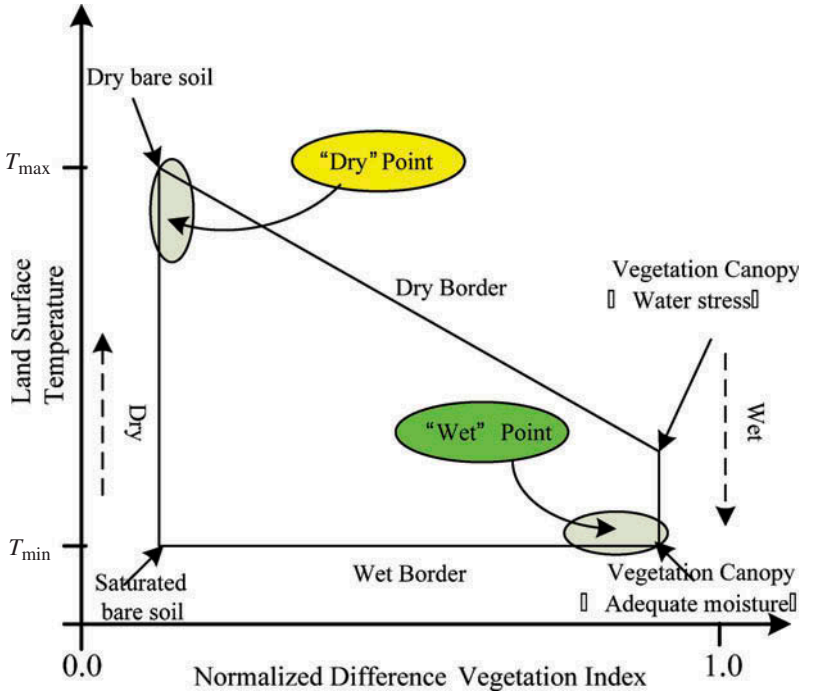


Figure 2. The spatial VITT configured by the NDVI and LST.

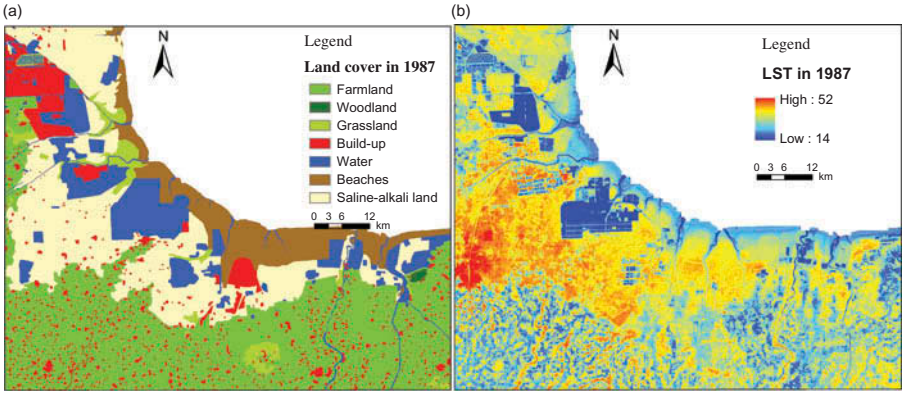


Figure 3. The spatial distribution of the (a) LUCC and (b) LST.

rural residential areas and other constructed land) accounted for 12.6% of the total area, and beach land accounted for only 3.2% of the total area. Thus, there are four major types of land-cover, that is, farmland, saline-alkali land, built-up land and water body, which together accounted for 95% of the total study area.

The changes in the land cover profoundly affect not only the changes in the vegetation index but also the changes of LST. The average LST of this study area is 30.8°C, and from Figure 3, we can observe that the regions of lower surface temperature are primarily

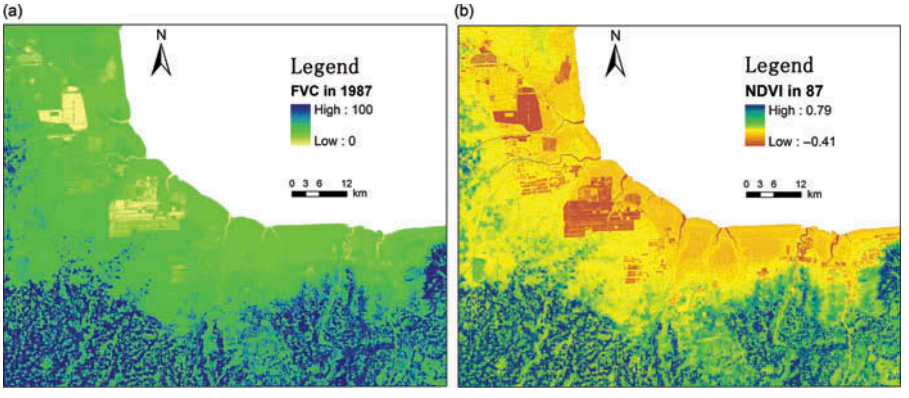


Figure 4. The spatial distribution of the (a) FVC and (b) NDVI.

distributed in the coastal beaches and water bodies, and the higher temperature regions are primarily distributed over the saline-alkali and built-up land. The LST is lower for the farmlands and grasslands.

Because the dominant land cover types of this study area are farmland, saline-alkali land, built-up land and water bodies, the average NDVI is 0.246 and the mean of the FVC is 32.4%. Figure 4 shows that the NDVI and FVC are lower in the areas covered by coastal beaches, saline-alkali land and water bodies and are higher in the areas covered by farmland and grassland.

Based on the SEBAL model (Bastiaanssen, Menenti, and Feddes 1998; Bastiaanssen, Pelgrum, and Wang 1998), with particular consideration of complex terrain features, the daily ET was estimated with the Landsat TM data collected on 7 May 1987.

From Figure 5, we observe that the average ET of the study area is 1.95 mm day$^{-1}$. Because the spatial variation of the ET is also affected by the obvious changes of land cover types, the larger ET value is primarily distributed in the coastal beaches and water bodies. The smaller ET value is primarily distributed in the areas of farmland, grassland and other regions covered with vegetation. The minimum ET value is distributed over saline-alkali land and construction land.

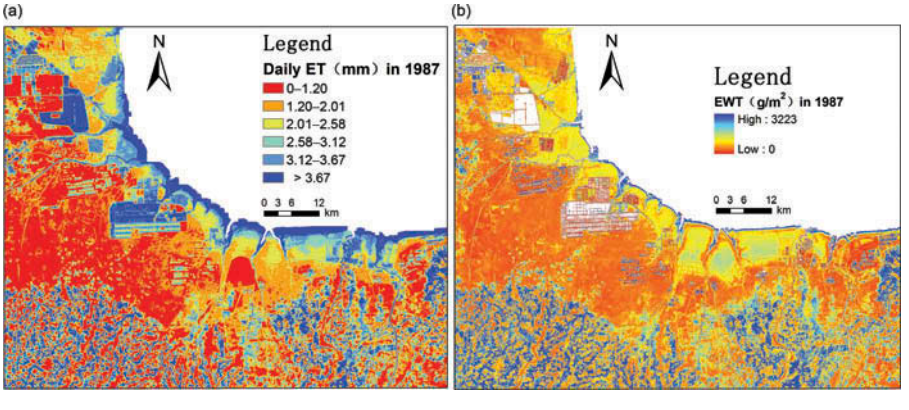


Figure 5. The spatial distribution of the (a) ET and (b) EWT.

Downloaded by [National Science Library] at 18:15 04 August 2015

The spatial distribution of the EWT is closely related to the surface vegetation. As shown in Figure 5, the average EWT of the study area is 515 g/m$^2$; the EWT is higher in the coastal regions covered by waters, crops and grass; and the highest EWT is 3233 g/m$^2$. Because the vegetation density directly affects the EWT, the EWT is lower in saline-alkali land that includes a certain amount of vegetation and is equal to 0 in the vegetation-free areas, including the built-up, shoals, and saline-alkali land.

The RWSI and TVDI are two drought-monitoring indices calculated using different methods. The RWSI is an index for monitoring the regional drought from calculations of the sensible heat, the net radiation of land surface and the soil heat based on the SEBAL model. The RWSI is slightly affected by land cover conditions and soil background and is a comparatively independent and objective indicator. The TVDI is obtained via calculation of the spatial VITT, which is obviously affected by land cover conditions and soil background. The regions with high values of the RWSI and TVDI are severely drought-ridden, and those areas with lower values indicate the presence of less severe drought. From Figure 6, we observe that the regions with both a higher RWSI and higher TVDI are distributed in the saline-alkali land followed by grassland and farmland, and the regions with lower values are coastal beaches where drought is not a serious problem.

Examining the regional spatial water distribution monitored by the RWSI and TVDI as standards, we can compare with the spatial distribution of the EWT. The regions with higher EWT values are primarily covered by vegetation and the EWT values of other regions are lower, which is not consistent with the spatial water distribution monitored by the RWSI and TVDI; therefore, it is less accurate and reasonable to use the EWT to monitor regional drought. Because the EWT only reflects the vegetation water content and cannot reflect the soil moisture in the region, the EWT can be used to monitor vegetation water and does not reflect the soil water of non-vegetation area correctly.

### 3.2. *The analysis of spatial distribution characteristics and response for EWT*

The EWT is defined as the ratio of the vegetation water content (the difference between the fresh weight and dry weight) and the leaf area and is a method for retrieving the vegetation water directly. The greatest advantage is that this method has nothing to do with the vegetation type, and thus it can reflect the water content of the different vegetation types in the study area more objectively. Although the EWT is unconcerned

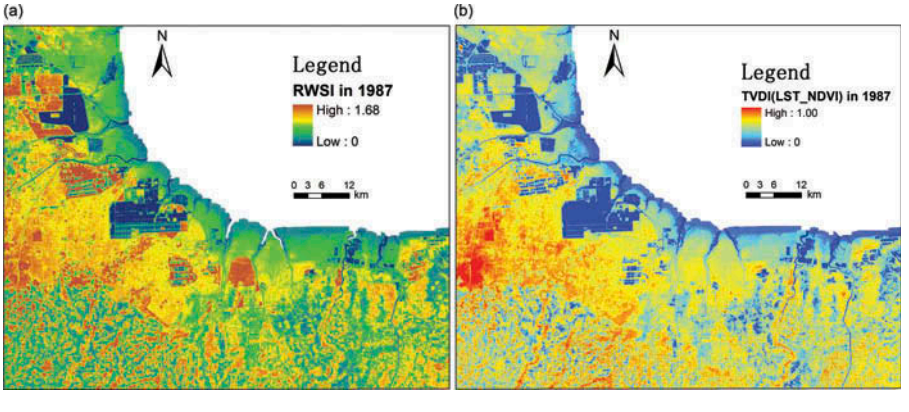


Figure 6. The spatial distribution of the (a) RWSI and (b) TVDI.

Downloaded by [National Science Library] at 18:15 04 August 2015

with vegetation types, it is closely related to the growing environment of the vegetation and relates not only to the regional topography, soil types, soil moisture and LST but also to the vegetation growth climate environment (precipitation and temperature), which obviously affects the EWT.

The LST and surface evapo-transpiration indicators (ET) corresponding to the space–time EWT were retrieved according to the relevant models. Next, the impacts of the LST and ET on the EWT and their correlations were analyzed. At the same time, the NDVI and FVC were retrieved for use in analysis of the impacts of surface vegetation density level on the EWT and their correlations.

The NDVI and the FVC are both remote sensing indices that reflect the vegetation density. A negative value of the NDVI means that a region has no vegetation covering, and the FVC is also equal to 0. When the NDVI is greater than 0, this indicates that the region is covered with vegetation and the FVC is also greater than 0. If the NDVI values increase, the FVC value also increases, which indicates an increase in the density of regional vegetation.

The indicative characteristics of the NDVI and FVC for the surface vegetation display a rather close relationship with the vegetation water content (EWT). We combined the EWT with the NDVI and FVC, and the corresponding EWT data were collected using an interval of 0.01 with the NDVI and FVC as independent variables to generate Figure 7, with which we analyzed the quantitative relationship between the vegetation index and EWT and its impact on the EWT.

As shown in Figure 7, the EWT presents different patterns of changes together with the changes in the NDVI (see Figure 7(a)) and FVC indices (see Figure 7(b)). When the NDVI shifts between 0 and 0.18 and the FVC shifts between 0 and 0.1, the EWT shows a decreasing trend, which indicates that the EWT has a negative correlation with the NDVI and FVC. The regions with an NDVI between 0 and 0.18 and an FVC between 0 and 0.1 are always in the state of changing from bare vegetation cover to sparse vegetation cover. These surfaces contain vegetation, but the vegetation cover is sparse. In this ecological environmental condition, the effect of the soil on the regional moisture and heat is far larger than that of the vegetation, and the EWT has a negative correlation with the NDVI and the FVC. Therefore, we observe that under the conditions of NDVI $< 0.18$ and FVC $< 0.1$, the vegetation coverage increases and the EWT decreases significantly. The negative correlation coefficients reach as high as 0.99, and the degree of negative correlation is notably high.

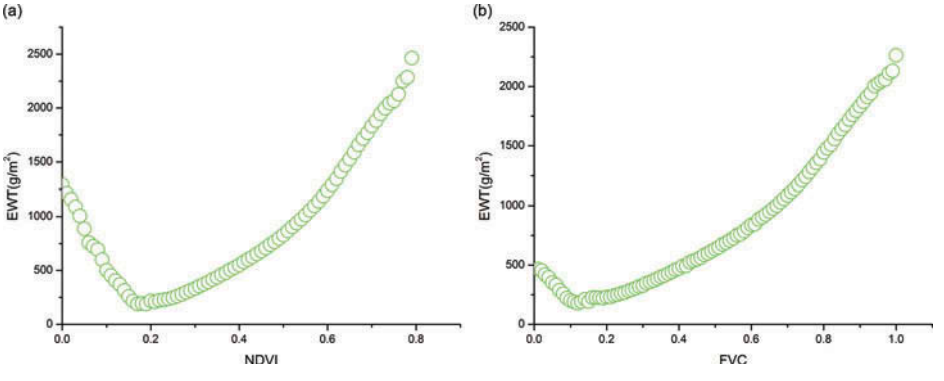


Figure 7. Changing graphs of the EWT with the (a) NDVI and (b) FVC.

Downloaded by [National Science Library] at 18:15 04 August 2015

When the NDVI is >0.18 and the FVC is >0.1, the vegetation coverage increases to a certain extent, and the effect of vegetation on the regional water and heat becomes larger than that of surface soil; in other words, the vegetation transpiration is greater than the evaporation. The EWT showed a significantly positive correlation with the NDVI and the FVC. The EWT also increases accordingly together with the increase in the NDVI and FVC indices. These indices showed a significant positive correlation, and their correlation coefficients were both 0.97.

From the above analysis, we observe that the changes in land coverage affect the EWT significantly. In an ecological environment with low vegetation coverage, the EWT changes produce negative relationships with the changes in vegetation density. When vegetation density increases to a certain extent, the EWT presents a significant positive correlation with the vegetation density.

The graph in Figure 8(a) illustrates the relationship of the LST and the EWT. As can be observed, when the LST is below 15°C, the land cover consists of beaches and water and contains no vegetation cover. When the LST is between 15°C and 25°C, the EWT shows an obvious increasing trend together with the increase in the LST, and a positive correlation exists between the EWT and LST. In this temperature range, vegetation transpiration and photosynthesis are gradually enhanced, and the vegetation water content also increases accordingly with the increase of the LST.

The LST at 25°C represents an inflection point and is also the most suitable temperature for vegetation photosynthesis. If the LST is >25°C, the vegetation water content gradually reduces along with the increasing LST.

Between 25°C and 35°C, the EWT reduces significantly with the increasing LST; the EWT is significantly influenced by the LST, and an obvious negative correlation exists between the EWT and LST. If the LST is >35°C, the EWT presents a slowly decreasing trend with the increase of the LST, which means that when the LST is >35°C, the vegetation loses a large amount of water through transpiration, and the vegetation water content is notably low. When the LST is >50°C, the vegetation exists in a state of withering or death.

From the above analysis, we observe that the LST has a significant impact on the vegetation water content and presents different relationships between the EWT and LST with varying LST. When the LST is <25°C, the EWT has a positive correlation with the LST. When the LST is >25°C, the EWT has a negative correlation with the LST.

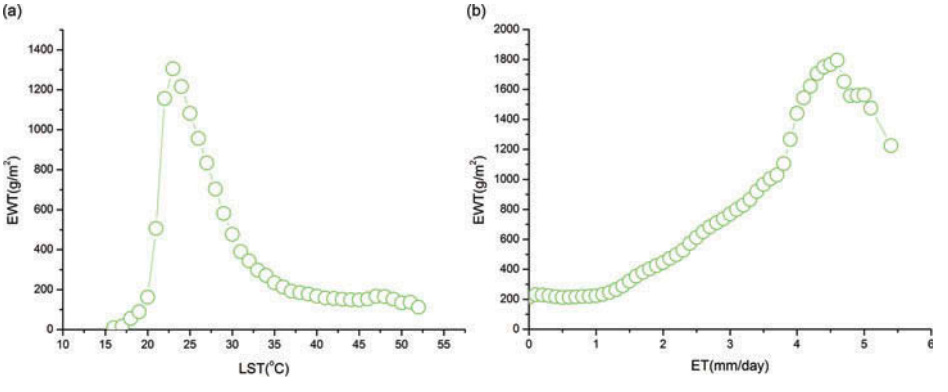


Figure 8. Changing graphs of the EWT with the (a) LST and (b) ET.

Downloaded by [National Science Library] at 18:15 04 August 2015

As shown in Figure 8(b), the ET of the ecological environment affects the vegetation water content significantly. In different intervals of ET, the correlation between the EWT and ET is also different. When the ET is <1 mm/day, the effect of the ET on EWT is small, and the EWT changes rather little with the increase of the ET.

When the ET is >1 mm/day and <4 mm/day, the EWT increases with the increase in the ET and a distinctly positive correlation exists between the EWT and ET with a correlation coefficient of 0.97. When the ET is between 4 and 5 mm/day, the EWT increases more significantly with the increase in the ET and a distinctly positive correlation between the EWT and ET.

If the ET is between 1 and 5 mm/day, a positive correlation exists between the EWT and ET, the vegetation water content is sufficient for transpiration and the EWT increases with the increase in ET.

If the ET is >5 mm/day, the surface evapo-transpiration is too strong and not enough vegetation water content exists for transpiration; the EWT falls sharply with the increase of the ET and forms a significant negative correlation the between the EWT and ET.

From the analysis in Figure 8, we observe that the ET of the ecological environment is closely related to the vegetation water content, and the EWT changes distinctly with different values of the ET. The changes of the ET affect the EWT significantly.

This analysis shows that the EWT is significantly affected by the vegetation cover density, as shown by the LST and ET. Under low-density vegetation coverage, a negative correlation exists between the EWT and the vegetation index (NDVI or FVC), and with high-density vegetation coverage, a positive correlation exists between the EWT and the vegetation index (NDVI or FVC).

When the LST is <25°C, the EWT is positively correlated with the LST, and if the LST is >25°C, a negative correlation exists between the EWT and LST. The ET of the ecological environment is closely related to the EWT. The EWT changes distinctly with different values of the ET such that the changes in the ET affect the EWT significantly.

### *3.3. The action of the EWT in monitoring of regional drought*

The ET of the land surface is an important measure for water loss and is closely related to the soil moisture conditions. Therefore, we can understand the changes in the soil moisture supply by monitoring the changes of the ET on the land surface, and monitoring for drought occurrence and development can provide a reliable basis for decision-making departments to enact timely and effective measures.

In this work, the RWSI was calculated with the SEBAL model as an indicator for regional drought monitoring. In formula (7), $H$ is the sensible heat flux, $Rn$ is the net radiation flux, $G$ is the soil heat flux and all of these parameters can be obtained from the SEBAL model. Therefore, the regional water stress could be monitored by coupling of the SEBAL model and remote sensing. We observe that the larger the RWSI, the more serious the water shortage, which is only a qualitative description of the soil water stress in these regions. To further determine the relationship between the RWSI and soil moisture, we need the observed values of soil moisture measured in the field to establish a regression model between the RWSI and soil moisture. Next, we will need to develop drought level indicators to monitor the regional drought conditions.

According to the research of other scholars, drought classification system was developed according to correlations between the relative soil moisture and the RWSI. The relative soil moisture and RWSI are two objective indicators in regional drought monitoring and reflect the gains and losses of regional water situation quite well (Table 1).

Downloaded by [National Science Library] at 18:15 04 August 2015

Table 1. Regional drought classification categories.

| Class | Relative soil moisture | RWSI | Drought level |
|---|---|---|---|
| 1 | <0.4 | >0.892 | Heavy drought |
| 2 | 0.4–0.5 | 0.752–0.892 | Medium drought |
| 3 | 0.5–0.6 | 0.612–0.752 | Light drought |
| 4 | 0.6–0.8 | 0.332–0.612 | Normal |
| 5 | >0.8 | <0.332 | Wet |

Note: *Relative soil moisture = soil moisture/soil saturation moisture × 100.

Downloaded by [National Science Library] at 18:15 04 August 2015

Vegetation water originates from the soil water of the land surface, and the soil water is derived from relatively stable groundwater and largely changeable precipitation. Because the precipitation condition is an important criterion of drought, the vegetation water content becomes an indirect indication of the local drought conditions. Therefore, the study of vegetation water content only can not only directly reflect the conditions of vegetation growth but also provide important reference information for drought and ecological security monitoring.

Combining the RWSI with the EWT and taking the RWSI as the standard and argument for drought monitoring, the correlation diagram between the EWT and RWSI was constructed as follows:

Figure 9 shows that when the RWSI is <0.2, the soil moisture exists in a relatively wet state according to the drought classification (RWSI < 0.332). In this area, the EWT has a positive correlation with the RWSI and the EWT will increase with the increasing RWSI.

When the RWSI is between 0.2 and 0.6, the soil moisture is in the normal state according to the drought classification, or in other words, the soil moisture is able to meet the demands of the vegetation for water, and the area will experience no drought. In this area, the EWT has a negative correlation with the RWSI, and the EWT will decrease with the increasing RWSI. The increasing RWSI means that the regional soil moisture is reduced and the EWT is also gradually reduced, which is consistent with the relationship between vegetation and soil moisture. The changes in the EWT can indicate the changes

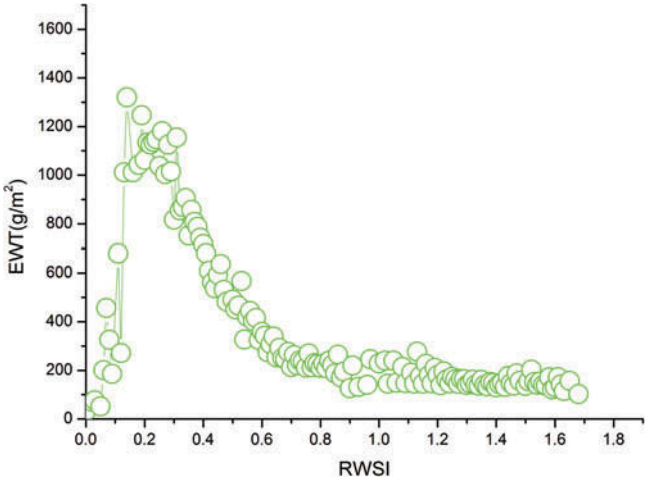


Figure 9. Correlation diagram between the EWT and RWSI.

in the regional soil moisture quite well and can act as an indicator and reference in regional drought monitoring.

When the RWSI is >0.6, the regional soil moisture begins to display mild and moderate drought conditions. Although the EWT also has a negative correlation with the RWSI, the EWT is reduced but decreases rather slowly, which indicates that when the regional soil water deficit reaches drought levels and the soil moisture is not sufficient to meet the demand of the vegetation, the vegetation will exist in a dry state and the action of the EWT for regional drought monitoring is not obvious.

From the above analysis we observe that although the EWT can monitor regional drought, its monitoring role is limited and the EWT is greatly affected by soil moisture. The EWT can indicate the changes in the regional soil water content, the presence of regional drought, and the gains and losses of soil moisture only when the soil water content is in a normal state (0.3–0.6). Because the region exists in the arid state, the EWT has no obvious indicator roles. Thus, the EWT is a conditional indicator of regional drought and has no significant effect for moderate to severe drought.

## 4. Conclusions

This article retrieved the EWT data from the near-infrared and shortwave infrared bands. False color composition was combined with the fourth, third, and second visible bands, and the land cover data were extracted with the aid of machine-assistant interpretation for use as a background for the related research.

At the same time, the NDVI and FVC were calculated using the infrared and near-infrared bands, and the LST was retrieved with a single-window algorithm (Qin, Karnieli, and Berliner 2001). The parameters of the surface net radiation (Rn), sensible heat (H), soil heat (Gn) and evapo-transpiration (ET) were calculated using the SEBAL model (Bastiaanssen, Menenti, and Feddes 1998; Bastiaanssen, Pelgrum, and Wang 1998). Furthermore, the RWSI was obtained according to the CWSI mechanism (Jackson and Idso 1981).

Using the analysis of the regional land cover status, the impacts of surface water heat flux and surface covering on the EWT were analyzed by combining the EWT with the vegetation index (NDVI and FVC) or the EWT with LST and ET. Finally, the roles and limitations of the EWT in drought monitoring were analyzed combined with the regional drought classification and the RWSI. From this analysis, the following conclusions can be drawn:

(1) The spatial distribution of the EWT is closely related to the land surface vegetation, and the density and sparse degree of vegetation cover affect the EWT directly. In regions with no vegetation cover (i.e., built-up land, shoals and saline-alkali soil), the EWT is nearly equal to 0.
(2) The EWT is affected significantly by the vegetation cover density, the LST and the ET. In the case of low vegetation coverage, the NDVI and FVC are negatively correlated with the EWT. Under conditions of high vegetation coverage, the NDVI and FVC are positively correlated with the EWT. When the LST is <25° C, the EWT is positively correlated with the LST and if the LST is >25°C, a negative correlation exists. The ET of the ecological environment is closely related to the vegetation water content. The vegetation water changes distinctly with different values of the ET, and thus the changes in the ET affect the EWT significantly.

Downloaded by [National Science Library] at 18:15 04 August 2015

(3) Although the EWT can monitor regional drought, its monitoring role is limited because it is greatly affected by the soil moisture. If the soil water is in a normal state (0.3–0.6), the EWT can act as a response and indicate the changes in the regional soil water, changes in the regional drought, and changes in the gains and losses in soil moisture. Because the region exists in an arid state, the EWT has no obvious indicator roles. Thus, the EWT is conditional for monitoring of regional drought and indicates no significant effect for moderate to severe drought.

## Funding

This work was supported by the Key Research Program of the Chinese Academy of Sciences [KZZD-EW-14], the Talent Fund of Yantai Institute of Coastal Zone Research [1106000004], the Ecological Innovation & Breeding Project [Y254021031 and Y355031061], the National Natural Science Foundation of China [41171334 and 41071278], the 6th special funding from China Postdoctoral Science Foundation [2013T60160] and the USDA NIFA Project [2010-34263-21075].

Downloaded by [National Science Library] at 18:15 04 August 2015

## References

Bastiaanssen, W. G. M., M. Menenti, and R. A. Feddes. 1998. "A Remote Sensing Surface Energy Balance Algorithm for Land (SEBAL) 1. Formulation." *Journal of Hydrology* 212–213: 198–212.

Bastiaanssen, W. G. M., H. Pelgrum, and J. Wang. 1998. "A Remote Sensing Surface Energy Balance Algorithm for Land (SEBAL). 2. Validation." *Journal of Hydrology* 212–213: 213–229.

Brown, J. F., B. D. Wardlow, T. Tadesse, M. J. Hayes, and B. C. Reed. 2008. "The Vegetation Drought Response Index (VegDRI): A New Integrated Approach for Monitoring Drought Stress in Vegetation." *GIScience & Remote Sensing* 45 (1): 16–46.

Cao, J. 2002. "Analysis of the Cause of Seawater Intrusion in Laizhou Bay of Shandong Province." *Journal of the Graduates, Sun Yat-Sen University (Natural Sciences, Medicine)* 23: 104–111.

Ceccato, P., S. Flasse, and J. M. Gregoire. 2002. "Designing a Spectral Index to Estimate Vegetation Water Content from Remote Sensing Data: Part 2. Validation and Applications." *Remote Sensing of Environment* 82: 198–207.

Ceccato, P., S. Flasse, S. Tarantola, S. Jacquemoud, and J. M. Gregoire. 2001. "Detecting Vegetation Leaf Water Content Using Reflectance in the Optical Domain." *Remote Sensing of Environment* 77: 22–33.

Ceccato, P., N. Gobron, S. Flasse, B. Pinty, and S. Tarantola. 2002. "Designing a Spectral Index to Estimate Vegetation Water Content from Remote Sensing Data: Part 1. Theoretical Approach." *Remote Sensing of Environment* 82: 188–197.

Chuvieco, E., D. Rian, I. Aguado, and D. Cocero. 2001. "Estimation of Fuel Moisture Content from Multitemporal Analysis of Landsat Thematic Mapper Reflectance Data: Applications in Fire Danger Assessment." *International Journal of Remote Sensing* 23 (11): 2145–2162.

Dawson, T. P., P. J. Curran, and S. E. Plummer. 1998. "LIBERTY—Modelling the Effects of Leaf Biochemistry on Reflectance Spectra." *Remote Sensing of Environment* 65: 50–60.

Finn, M. P., M. Lewis, D. D. Bosch, M. Giraldo, K. Yamamoto, D. G. Sullivan, R. Kincaid, R. Luna, G. Allam, C. Kvien, and M. S. Williams. 2013. "Remote Sensing of Soil Moisture Using Airborne Hyperspectral Data." *GIScience & Remote Sensing* 48 (4): 522–540.

Gao, B. C. 1996. "NDWI-a Normalized Difference Water Index for Remote Sensing of Vegetation Liquid Water From Space." *Remote Sensing of Environment* 58: 257–266.

Gao, Z., C. Liu, W. Gao, and N. B. Chang. 2010. "A Coupled Remote Sensing and the Surface Energy Balance with Topography Algorithm (SEBTA) to Estimate Actual Evapotranspiration Over Heterogeneous Terrain." *Hydrology and Earth System Sciences* 7: 4875–4924.

Gobron, N., B. Pinty, M. Verstraete, and Y. Govaerts. 1999. "The MERIS Global Vegetation Index (MGVI): Description and Preliminary Application." *International Journal of Remote Sensing* 20 (9): 1917–1927.

Gutman, G., and A. Ignatov. 1998. "The Derivation of the Green Vegetation F Raction F Rom NOAA/AVHRR Data for Use in Numerical Weather Prediction Models." *International Journal of Remote Sensing* 19 (8): 1533–1546.

Jackson, R. D., and S. B. Idso. 1981. "Canopy Temperature as a Crop Water Stress Indicator." *Water Resources* 17: 133–138.

Kaufman, Y. J., A. Karnieli, and D. Tanre. 2000. "Detection of Dust Over Deserts Using Satellite Data in the Solar Wavelengths." *IEEE Transactions on Geoscience and Remote Sensing* 38 (1): 525–531.

Kaufman, Y. J., and C. Sendra. 1988. "Algorithm for Automatic Atmospheric Corrections to Visible and Near-IR Satellite Imagery." *International Journal of Remote Sensing* 9 (8): 1357–1381.

Kaufman, Y. J., D. Tanré, L. A. Remer, E. F. Vermote, A. Chq, and B. N. Holben. 1997. "Operational Remote Sensing of Tropospheric Aerosol Over Land From EOS Moderate Resolution Imaging Spectroradiometer." *Journal of Geophysical Research* 102 (17): 51–68.

Liang, S., H. Fallah-Adl, S. Kalluri, J. JáJá, Y. J. Kaufman, and J. R. G. Townshend. 1997. "An Operational Atmospheric Correction Algorithm for Landsat Thematic Mapper Imagery Over the Land." *Journal of Geophysical Research* 102 (D14): 17173–17186.

Liang, S., H. Fang, and M. Chen. 2001. "Atmospheric Correction of Landsat ETM+ Land Surface Imagery. I. Methods." *IEEE Transactions on Geoscience and Remote Sensing* 39 (11): 2490–2498.

Liang, S., H. L. Fang, J. T. Morisette, M. Z. Mingzhen Chen, C. J. Shuey, C. L. Walthall, and C. S. T. Daughtry. 2002. "Atmospheric Correction of Landsat ETM+ Land Surface Imagery. II. Validation and Applications." *IEEE Transactions on Geoscience and Remote Sensing* 40 (12): 2736–2746.

Moghaddam, M., and S. Saatchi. 1999. "Monitoring Tree Moisture Using an Estimation Algorithm Applied to SAR Data From BOREAS." *IEEE Transactions on Geoscience and Remote Sensing* 17 (2): 901–916.

Peng, G., Y. Chen, and J. Li. 2007. "The Research on Forest Fire Monitoring Combined with Remote Sensing Data and Meteorological Data – Take Malaysia Peninsula as an Example." *Geo-Information Science* 9 (5): 99–103.

Qin, Z., A. Karnieli, and P. Berliner. 2001. "A Mono-Window Algorithm for Retrieving Land Surface Temperature from Landsat TM Data and Its Application to the Israel–Egypt Border Region." *International Journal of Remote Sensing* 22 (18): 3719–3746.

Rouse, J. W., R. H. Haas, J. A. Schell, and D. W. Deering. 1973, "Monitoring Vegetation Systems in the Great Plains with ERTS," *Third ERTS Symposium,* NASA SP-351 I: 309–317.

Sandholt, I., K. Rasmussen, and J. Andersen. 2002. "A Simple Interpretation of the Surface Temperature/Vegetation Index Space for Assessment of Surface Moisture Status." *Remote Sensing of Environment* 79: 213–224.

Tucker, C. J. 1977. "Asymptotic Nature of Grass Canopy Spectral Reflectance." *Applied Optics* 16 (5): 1151–1156.

Tucker, C. J. 1979. "Red and Photographic Infrared Linear Combinations for Monitoring Vegetation." *Remote Sensing of Environment* 8: 127–150.

Wang, J., R. Xu, and Y. Ma. 2008. "The Remote Sensing Method of Retrieving Vegetation Water Content and Research Progress." *Remote Sensing Information* 1: 100–105.

Wang, Q., Z. Ren, and G. Sun. 2002. "Research on Seawater Intrusion Disaster in South-East Coastwise Area of Laizhou Bay." *Marine Environmental Science* 21: 10–13.

Downloaded by [National Science Library] at 18:15 04 August 2015